10.24425/119079

Archives of Control Sciences
Volume 28(LXIV), 2018
No. 1*, pages 105–118*

Application of predictive control for manipulator mounted on a satellite

TOMASZ RYBUS, KAROL SEWERYN and JUREK Z. SĄSIADEK

Specific conditions of on-orbit environment are taken into account in the design of all devices intended to be used in space. Despite this fact malfunctions of satellites occur and sometimes lead to shortening of the satellite operational lifetime. It is considered to use unmanned servicing satellite, that could perform repairs of other satellites. Such satellites equipped with a manipulator, could be used to capture and remove from orbit large space debris. The critical part of planned missions is the capture manoeuvre. In this paper a concept of the control system for the manipulator mounted on the satellite is presented. This control system is composed of the trajectory planning module and model predictive controller (the latter is responsible for ensuring precise realization of the planned trajectory). Numerical simulations performed for the simplified planar case with a 2 DoF manipulator show that the results obtained with the predictive control are better than the results obtained with adaptive control method.

Key words: space robotics, predictive control, trajectory optimization, free-floating manipulator.

1. Introduction

All devices intended to be used on-orbit must be prepared to operate in a very demanding environment (radiation, high vacuum, microgravity). Moreover, every payload is subjected to high dynamic loads in the launch phase. Specific conditions of the orbital environment must be taken into account in the design phase, space certified components are used and all devices are rigorously tested on the ground before launch [4]. Nevertheless, malfunctions during the orbital operations do occur and may lead to shortening of the satellite operational lifetime [2]. Repairs carried on orbit are among several types of operations classified as on-orbit satellite servicing [18]. Up to now such repairs were performed extremely rarely and always by astronauts. Alternative solution is to perform unmanned servicing missions with the use of autonomous servicing vehicles.

T. Rybus (the corresponding author) and K. Seweryn are with Space Research Centre (CBK PAN), Bartycka 18a, Warsaw, Poland, e-mail: trybus@cbk.waw.pl.

J.Z. Sąsiadek is with Department of Mechanical and Aerospace Eng., Carleton University, Ottawa, Ontario, Canada.

Received 26.01.2017. Revised 9.02.2018.

In the planned servicing missions it is frequently assumed that the target object is not equipped with a dedicated docking mechanism and that this target object is uncontrolled (e.g., due to the malfunction of the attitude control system). In such cases it is considered to use a chaser satellite equipped with a manipulator. A gripper is mounted at the end of the manipulator to catch the selected element of the target object. Such unmanned manipulator-equipped satellite could also be used to catch space debris (e.g., spend rocket stages, defunct satellites) [16]. Space debris pose a real threat to active satellites and manned orbital flights. Therefore, several different options are considered to actively remove large space debris from an orbit (such planned actions are called Active Debris Removal, ADR).

Technologies required to perform the orbital capture manoeuvre are being developed. Several technology demonstration missions were performed to test selected technologies (e.g., ETS-VII [8]). In these missions the target object was controlled and was equipped with the capture interface. Using manipulator to grasp an uncontrolled object is a much difficult task. One of the biggest challenges is to develop a control system for the manipulator-equipped servicing satellite. In this paper we focus on the control of such satellite. Broad review of control methods for orbital manipulators can be found in [3]. In our earlier paper we have proposed a concept of a control system composed of two modules [9]. One module is responsible for the manipulator trajectory planning, while the second module is responsible for trajectory following during the motion of the manipulator. In [10] we have shown that the trajectory following module can be based on a predictive control algorithm that uses full non-linear model of the satellite-manipulator system. The application of the predictive control for a manipulator mounted on a satellite is not a new idea, but authors of previous works devoted to this subject have made significant simplifying assumptions (e.g., the linearization of the dynamic model of the system or the assumption that the servicing satellite is fixed during the capture manoeuvre [7]). The predictive control, in comparison to other control methods, is characterized by a high precision of trajectory following. Moreover, in the predictive control future state of the system is predicted and this control method takes into account the fact that the reference trajectory (provided by the trajectory planning module) is known in advance.

This paper is based on a paper presented at the 14th National Conference on Robotics that took place in Polanica Zdrój, Poland, in 2016 [11]. Large part of this paper is also based on our two previous articles: [9] and [10]. There are two new elements, presented in [11], but not in [9] and [10]. First, results obtained with the Non-linear Model Predictive Control (NMPC) are compared with the Simple Modified Adaptive Control (MSAC) [17], that also takes into account the full non-linear model of the satellite-manipulator system (in this case the dynamic Jacobian has been used [13]). The second new element is the comparison of control torques obtained with different control methods. Analysis of the con-

trol effort allows the reader to clearly seen the advantages of model predictive control. These two elements are the main contribution of this paper.

Dynamic equations of the satellite-manipulator system are presented in section 2, while the proposed control system is presented in section 3 (with focus on the trajectory following module). Results of numerical simulations are provided in section 4. Conclusions are presented in section 5.

2. Dynamic equations of the satellite-manipulator system

We are considering a satellite that is equipped with a manipulator that has n rotational degrees of freedom (Fig. 1). The equations presented in this section are given in the inertial reference frame $x_i\, y_i\, z_i$. These equations were previously presented in [10], while they complete derivation can be found in [14].

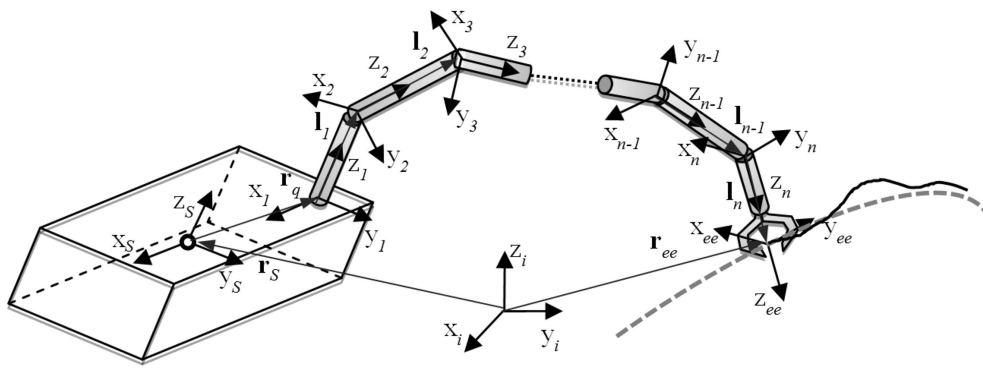

Figure 1: The schematic view of a chaser satellite equipped with a manipulator

To describe the satellite-manipulator system we use generalized coordinates in the following form [5]:

$$\boldsymbol{q}_p = [\boldsymbol{r}_s^T \quad \boldsymbol{\Theta}_s^T \quad \boldsymbol{\theta}^T]^T, \tag{1}$$

where $\boldsymbol{r}_s$ denotes the satellite centre of mass, $\boldsymbol{\Theta}_s$ denotes the satellite orientation, and $\boldsymbol{\theta}$ is the n-dimensional vector that contains positions of manipulator joints. Euler angles are used to describe the orientation of the satellite, because their use is more intuitive than the use of quaternions. Moreover, in the considered manoeuvres changes of satellite orientation are small (there is no risk of obtaining a singular configuration). The generalized equation of motion of the satellite-manipulator system can be presented as:

$$\boldsymbol{M}(\boldsymbol{q}_p)\ddot{\boldsymbol{q}}_p + \boldsymbol{C}\left(\dot{\boldsymbol{q}}_p, \boldsymbol{q}_p\right)\dot{\boldsymbol{q}}_p = \boldsymbol{Q}, \tag{2}$$

where $\boldsymbol{M}(\boldsymbol{q}_p)$ denotes the generalized mass matrix, $\boldsymbol{C}(\dot{\boldsymbol{q}}_p, \boldsymbol{q}_p)$ denotes the Coriolis matrix, while $\boldsymbol{Q}$ is the vector of generalized forces. There is no vector of potential forces in equation (2), because the satellite on orbit is in a state of free-fall. Matrix $\boldsymbol{M}(\boldsymbol{q}_p)$ can be presented as:

$$\boldsymbol{M}(\boldsymbol{q}_p) = \begin{bmatrix} \boldsymbol{A} & \boldsymbol{B} & \boldsymbol{D} \\ \boldsymbol{B}^T & \boldsymbol{E} & \boldsymbol{F} \\ \boldsymbol{D}^T & \boldsymbol{F}^T & \boldsymbol{N} \end{bmatrix}. \tag{3}$$

Matrices $\boldsymbol{A}$, $\boldsymbol{B}$, $\boldsymbol{D}$, $\boldsymbol{E}$, $\boldsymbol{F}$ and $\boldsymbol{N}$ are defined as follows [14]:

$$\boldsymbol{A} = \left(m_s + \sum_{i=1}^{n} m_i \right) \boldsymbol{I}, \tag{4}$$

$$\boldsymbol{B} = \left(m_s + \sum_{i=1}^{n} m_i \right) \widetilde{\boldsymbol{r}}_{s\_g}, \tag{5}$$

$$\boldsymbol{D} = \sum_{i=1}^{n} m_i \boldsymbol{J}_{Ti}, \tag{6}$$

$$\boldsymbol{E} = \boldsymbol{I}_s + \sum_{i=1}^{n} \left(\boldsymbol{I}_i + m_i \widetilde{\boldsymbol{r}}_{i\_s}^T \widetilde{\boldsymbol{r}}_{i\_s} \right), \tag{7}$$

$$\boldsymbol{F} = \sum_{i=1}^{n} (\boldsymbol{I}_i \boldsymbol{J}_{Ri} + m_i \widetilde{\boldsymbol{r}}_{i\_s} \boldsymbol{J}_{Ti}), \tag{8}$$

$$\boldsymbol{N} = \sum_{i=1}^{n} \left(\boldsymbol{J}_{Ri}^T \boldsymbol{I}_i \boldsymbol{J}_{Ri} + m_i \boldsymbol{J}_{Ti}^T \boldsymbol{J}_{Ti} \right), \tag{9}$$

where $\boldsymbol{r}_{s\_g} = \boldsymbol{r}_s - \boldsymbol{r}_g$, $\boldsymbol{r}_{i\_s} = \boldsymbol{r}_i - \boldsymbol{r}_s$, $\boldsymbol{r}_i$ denotes the position of the i-th kinematic pair of the manipulator in respect to the $i-1$ pair, symbol ~ denotes matrix which is equivalent of a vector cross-product, m_s is the chaser satellite mass, while $\boldsymbol{I}_s$ is its mass moment of inertia tensor, m_i is the mass of i-th manipulator link, while $\boldsymbol{I}_i$ is the mass moment of inertia tensor of this link, $\boldsymbol{1}$ denotes the unity matrix, $\boldsymbol{J}_{Ti}$ is the translational component of the manipulator Jacobian, while $\boldsymbol{J}_{Ri}$ is the rotational component of this Jacobian. Jacobian ($6 \times n$ matrix) is given in the inertial reference frame. Components of the Coriolis matrix are computed from:

$$C_{ij} = \sum_{k=1}^{n} \left(\frac{d}{d(q_p)_k} m_{ij} - \frac{1}{2} \frac{d}{d(q_p)_i} m_{jk} \right), \tag{10}$$

where $m_{ij} \in \boldsymbol{M}(\boldsymbol{q}_p)$, while $i,\ j,\ k = 1, \ldots, n$. In equation (10) $(q_p)_k$ denotes the k-th element of the generalized coordinates vector $\boldsymbol{q}_p$, while $(q_p)_i$ denotes i-th

element of this vector. Vector of generalized forces $\mathbf{Q}$ can be presented as:

$$\boldsymbol{Q} = \begin{bmatrix} \boldsymbol{F}_s^T & \boldsymbol{H}_s^T & \boldsymbol{u}^T \end{bmatrix}^T, \tag{11}$$

where $\boldsymbol{F}_s$ denotes the external forces acting on the satellite, $\boldsymbol{H}_s$ denotes the external torques acting on the satellite, while $\boldsymbol{u}$ is the n-dimensional vector that contains the control torques applied in manipulator joints. The approach presented herein is general and allows analysis of system with non-zero and time-varying momentum and angular momentum [14]. However, for the purpose of the control system analysis, we take the simplifying assumption that there are no external forces and torques acting on the system, i.e., $\boldsymbol{F}_s = 0$ and $\boldsymbol{H}_s = 0$. In the short time scale of the capture manoeuvre this assumption is justified. We also assume that the manipulator-equipped satellite is not using its thrusters and momentum wheels during the motion of the manipulator.

3. Control system

3.1. General concept of the control system

In this section we present a concept of the control system for the manipulator mounted on the satellite that is based on the concept that we have presented in [9]. Control system of the manipulator is responsible for two tasks: (i) planning trajectory of the manipulator and (ii) ensuring realization of selected trajectory. This concept is shown in Fig. 2. The planned trajectory can be defined in the configuration space of the manipulator or as an end-effector trajectory given in the Cartesian space. Trajectories defined in the configuration space are only useful during very simple manoeuvres (e.g., unfolding of the manipulator). During the capture manoeuvre it is necessary to control the position of the end-effector in respect to the target object. When the planned trajectory is executed control system must minimize the difference between the current end-effector position and the end-effector position on the reference trajectory. Ensuring realization of a trajectory defined in the Cartesian space is more difficult than controlling the manipulator in the configuration space, because in such case Jacobian must be used to convert end-effector velocity to velocities of the manipulator joints.

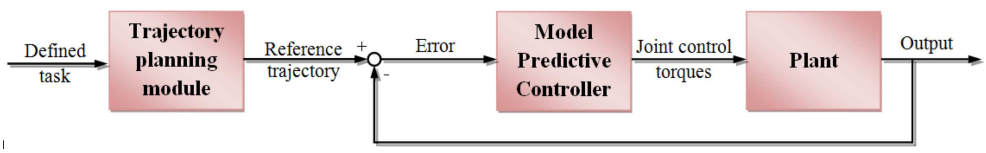

Figure 2: Concept of the control system for the manipulator mounted on the satellite (this picture is based on [9])

In the case considered herein, in which the manipulator is mounted on the satellite, motion of the manipulator influence position and orientation of the satellite. This fact was taken into account in equations presented in section 2 (alternatively, the dynamic Jacobian can be used [13]).

The control torque applied in the manipulator joints could be presented as a sum of the reference control torque $\boldsymbol{u}_{ref}$ (computer during the trajectory planning stage) and the control torque $\boldsymbol{u}_{contr}$ that is generated by the controller during the realization of the trajectory. Control torque $\boldsymbol{u}_{contr}$ depends on the error in trajectory realization. Thus, for the case of trajectory defined in the configuration space of the manipulator we can use the following equation:

$$\boldsymbol{u} = \boldsymbol{u}_{ref} + \boldsymbol{u}_{contr}\left(\boldsymbol{e}_{\boldsymbol{\theta}}, \boldsymbol{e}_{\dot{\boldsymbol{\theta}}}\right) \tag{12}$$

while for the case of the end-effector trajectory defined in the Cartesian space the following expression is used:

$$\boldsymbol{u} = \boldsymbol{u}_{ref} + \boldsymbol{u}_{contr}\left(\boldsymbol{e}_{p}, \boldsymbol{e}_{v}\right), \tag{13}$$

where: $\boldsymbol{e}_{\boldsymbol{\theta}} = \boldsymbol{\theta} - \boldsymbol{\theta}_{ref}$, $\boldsymbol{e}_{\dot{\boldsymbol{\theta}}} = \dot{\boldsymbol{\theta}} - \dot{\boldsymbol{\theta}}_{ref}$, $\boldsymbol{e}_{p} = \boldsymbol{r}_{ee} - (\boldsymbol{r}_{ee})_{ref}$, $\boldsymbol{e}_{v} = \boldsymbol{v}_{ee} - (\boldsymbol{v}_{ee})_{ref}$, $\boldsymbol{r}_{ee}$ denotes the end-effector position, while $\boldsymbol{v}_{ee}$ denotes its velocity. The subscript *ref* denotes the reference trajectory. Computation of the reference control torque $\boldsymbol{u}_{ref}$ in the trajectory planning stage is not necessary. The controller should be able to generate the appropriate control torque during the realization of the reference trajectory.

3.2. Trajectory planning module

Presented trajectory planning module is described in details in our previous paper [12]. This module is responsible for designing such a trajectory of the manipulator that will allow fulfilment of a defined task (e.g., unfolding of the manipulator). Planning a trajectory that will allow grasping of the target object is the most difficult task. In such case knowledge of the target object position, orientation and velocity is required (these information could be obtained, e.g., from a visual motion recognition system). Obstacles in the manipulator workspace (e.g., solar panels) must be taken into account during the trajectory planning. Moreover, obtained trajectory must not be close to the singular configurations of the manipulator.

There are several methods that could be used for planning trajectory of the manipulator mounted on the satellite. Optimization methods are especially important, because they allow, e.g., to minimize the influence of manipulator motion on the chase satellite position and orientation [6] or they can be used to minimize the control torques applied in the manipulator joints [15]. In our approach we have implemented the optimization algorithm presented in [12]. This

algorithm allows minimization of a quadratic norm connected with the power use of manipulator motors.

The optimized functional G has the following form:

$$G\left(\boldsymbol{q}_{vp}(t),\boldsymbol{u}(t),t\right)=\int_{t_0}^{t_f} L_k\left(\boldsymbol{q}_{vp}(t),\boldsymbol{u}(t),t\right)+\boldsymbol{\lambda}_{vp}(t)^T\boldsymbol{g}\left(\boldsymbol{q}_{vp}(t),\boldsymbol{u}(t),t\right)dt, \quad (14)$$

where: L_k denotes the selected cost function, $\boldsymbol{q}_{vp}$ denotes a vector composed from the generalized coordinates $\boldsymbol{q}_p$ and their first derivatives in respect to time $\left(\boldsymbol{q}_{vp}=\left[\boldsymbol{q}_v^T\ \ \boldsymbol{q}_p^T\right]^T\right)$, $\boldsymbol{\lambda}_{vp}$ is the vector composed of Lagrange multipliers (related to $\boldsymbol{q}_{vp}$). Function $\boldsymbol{g}$ in equation (14) describes the dynamics of the satellite-manipulator system:

$$\boldsymbol{g}=\begin{bmatrix}\dot{\boldsymbol{q}}_v\\ \dot{\boldsymbol{q}}_p\end{bmatrix}=\begin{bmatrix}\boldsymbol{M}^{-1}\left(\boldsymbol{q}_p\right)\left[\boldsymbol{Q}-\boldsymbol{C}\left(\dot{\boldsymbol{q}}_p,\boldsymbol{q}_p\right)\boldsymbol{q}_v\right]\\ \boldsymbol{q}_v\end{bmatrix}. \quad (15)$$

We use the following quadratic norm as a cost functional that is minimized:

$$L_k=\frac{1}{2}\boldsymbol{u}^T\boldsymbol{u}. \quad (16)$$

Hamiltonian of the system is given by:

$$H=L_k+\boldsymbol{\lambda}_{vp}^T\boldsymbol{g}. \quad (17)$$

Condition: $\dfrac{\partial H}{\partial \boldsymbol{u}}=0$ is used to find extremum of G. This condition allow us to find the control torque vector $\boldsymbol{u}$. Trajectory planning is performed before the motion of the manipulator begins. Thus, trajectory planning algorithm can have a high computational cost. In the ideal case (no disturbances, perfect knowledge of system mass and geometrical properties) control torques computed in the trajectory planning stage would be sufficient to perform the planned motion of the manipulator without the use of any controller.

3.3. Model predictive controller

The controller must be used during the motion of the manipulator to ensure realization of the selected reference trajectory. Various control algorithms could be used for this purpose [3]. In the presented concept of the control system we propose use of the NMPC [1]. Structure of this controller is presented in Fig. 3.

The technique of Model Predictive Control (MPC) is based on a model of the system that is used to obtain the control signal by minimizing selected objective

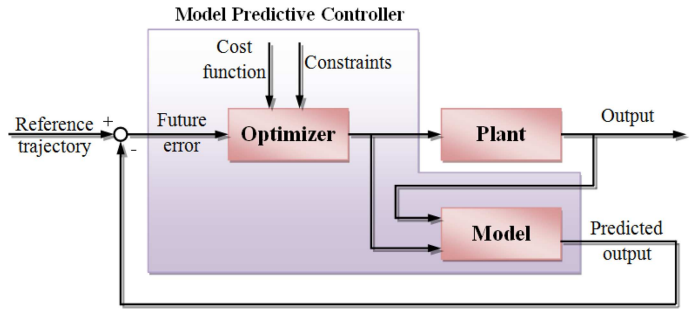

Figure 3: Structure of the predictive controller (this picture is based on [9])

function (in our approach we have chosen the minimization of Least Squares Term, LSQ). The model of the system is used to predict state of the system at future time instants (horizon). At each instant the first control signal of the sequence is applied to the system and the horizon is displaced towards the future. Receding strategy is employed [1].

The following state vector is used when the reference trajectory is defined in the configuration space:

$$\boldsymbol{x} = \boldsymbol{q}_{vp} = \left[\boldsymbol{v}_s^T \;\; \boldsymbol{\omega}_s^T \;\; \dot{\boldsymbol{\theta}}^T \;\; \boldsymbol{r}_s^T \;\; \boldsymbol{\Theta}_s^T \;\; \boldsymbol{\theta}^T\right]^T, \tag{18}$$

where $\boldsymbol{v}_s$ denotes the linear velocity of the manipulator-equipped satellite centre of mass, $\boldsymbol{\omega}_s$ denotes the angular velocity of the satellite, while $\dot{\boldsymbol{\theta}}$ denotes the first derivative in respect to time of the positions of manipulator joints (i.e., $\dot{\boldsymbol{\theta}}$ denotes the velocities of manipulator kinematic pairs). Set of equations (15) is used for simulation of the real satellite-manipulator system and as a model of this system in the NMPC.

For the case of a reference end-effector trajectory defined in the Cartesian space it is necessary to add end-effector position $\boldsymbol{r}_{ee}$ to the state vector:

$$\boldsymbol{x}_e = \left[\boldsymbol{v}_s^T \;\; \boldsymbol{\omega}_s^T \;\; \dot{\boldsymbol{\theta}}^T \;\; \boldsymbol{r}_s^T \;\; \boldsymbol{\Theta}_s^T \;\; \theta^T \;\; \boldsymbol{r}_{ee}^T\right]^T. \tag{19}$$

The current end-effector position is computed in every state from the remaining components of the state vector (the position of the end-effector in the inertial reference frame depends not only on the positions of manipulator joints, but also on the position and orientation of the chaser satellite). As in our earlier studies, in the numerical simulations we have used ACADO Toolkit implementation of the predictive controller.

4. Validation of the control system

At this early stage of the control system development it seems justified to focus on the simplified planar case, in which the satellite is equipped with a manipulator that has 2 DoF. It is planned to test the proposed control system on the planar air-bearing microgravity simulator at the Space Research Centre of the Polish Academy of Sciences (CBK PAN). This test-bed allows simulation of microgravity conditions in one plane. Thus, results of the numerical simulations presented in this paper for the planar case, could be later compared with the results of experiments. It is a common approach in space robotics to perform the preliminary analysis for the planar case only (e.g., [7, 17]). Detailed analysis of the proposed control system require to perform the numerical simulations with several different reference trajectories and with different disturbances acting on the system. Some analysis were already performed and their results were presented in [9]. In this paper we focus on the comparison of the results obtained using the NMPC with the results obtained using a Modified Simple Adaptive Control (MSAC) [17]. In the adaptive control method the control torque is computed with the following equation:

$$\boldsymbol{u}_{contr} = \boldsymbol{J}_M^{-1} \left(\boldsymbol{K}_p \boldsymbol{e}_p - \boldsymbol{K}_d \boldsymbol{e}_v \right), \tag{20}$$

where $\boldsymbol{J}_M$ denotes the geometric Jacobian of the manipulator, while $\boldsymbol{K}_p$ and $\boldsymbol{K}_d$ denote the adapted control gains given with the equations presented in [17]. In the equation (20) the dynamic Jacobian $\boldsymbol{J}_{Dyn}$ [13] could be used instead of $\boldsymbol{J}_M$. The dynamic Jacobian takes into account the fact that the manipulator base is free to move and rotate:

$$\boldsymbol{J}_{Dyn} = \boldsymbol{J}_M - \boldsymbol{J}_S \boldsymbol{H}_2^{-1} \boldsymbol{H}_3, \tag{21}$$

where $\boldsymbol{J}_S$ denotes the Jacobian of the satellite, while matrices $\boldsymbol{H}_2$ and $\boldsymbol{H}_3$ are defined as follows:

$$\boldsymbol{H}_2 = \begin{bmatrix} \boldsymbol{A} & \boldsymbol{B} \\ \boldsymbol{B}^T + \widetilde{\boldsymbol{r}}_s \boldsymbol{A} & \boldsymbol{E} + \widetilde{\boldsymbol{r}}_s \boldsymbol{B} \end{bmatrix}, \tag{22}$$

$$\boldsymbol{H}_3 = \begin{bmatrix} \boldsymbol{D} \\ \boldsymbol{F} + \widetilde{\boldsymbol{r}}_s \boldsymbol{D} \end{bmatrix}. \tag{23}$$

With the dynamic Jacobian we can formulate the following relation:

$$\dot{\boldsymbol{\theta}} = \boldsymbol{J}_{Dyn}^{-1} \begin{bmatrix} \boldsymbol{v}_{ee} \\ \boldsymbol{\omega}_{ee} \end{bmatrix}. \tag{24}$$

Moreover, we can use inverse of the Jacobian instead of the Jacobian transpose to obtain higher accuracy, but the computational cost will also be higher.

In our numerical simulations we have used mass and geometrical properties of the satellite-manipulator system used on the test-bed at CBK PAN: $m_s = 12.9$ kg, $I_s = 0.208$ kg·m^2, $\boldsymbol{r}_q = [0.327m \;\; 0]$, $m_1 = 4.5$ kg, $I_1 = 0.32$ kg$\cdot$m^2, $l_1 = 0.62$ m, $m_2 = 1.5$ kg, $I_2 = 0.049$ kg$\cdot$m^2, $l_2 = 0.6$ m. In this paper we present results obtained for an end-effector reference trajectory defined in the Cartesian space, as this is the more challenging case. We select a square as a reference trajectory. The square trajectory is especially difficult for the control system, because of the sharp corners. Such reference trajectory is commonly used to test control systems for manipulators (e.g., [17]). We have chosen a square with a side equal to 0.2 m. The initial state of the system is: $\boldsymbol{x}_e = [0\ 0\ 0\ 0\ 0\ 0\ 0\ 0\ 0.4\ -0.2\ 1.49$ m $0.36m]^T$. In the considered case we are only interested in ensuring the proper trajectory realization of the end-effector. Thus, the following LSQ matrix was selected: $\boldsymbol{W} = diag(0\ 0\ 0\ 0\ 0\ 0\ 0\ 0\ 0\ 0\ 10\ 10)$. Length of the prediction horizon and number of control intervals were selected in the numerical simulations. In the results presented in this section the length of the prediction horizon is 1 s, while the number of control intervals is 20. The maximal control torques that can be applied in the manipulator joints were set to 50 Nm.

Position of the end-effector during realization of the reference trajectory is presented in Fig. 4, while difference between the reference end-effector position and position obtained in the numerical simulations is presented in Fig. 5. The control torque applied in the first joint of the manipulator is presented in Fig. 6. In Fig. 7 this torque was presented for the motion of the end-effector through the first corner of the square reference trajectory. Control torque applied in the second joint of the manipulator is very similar.

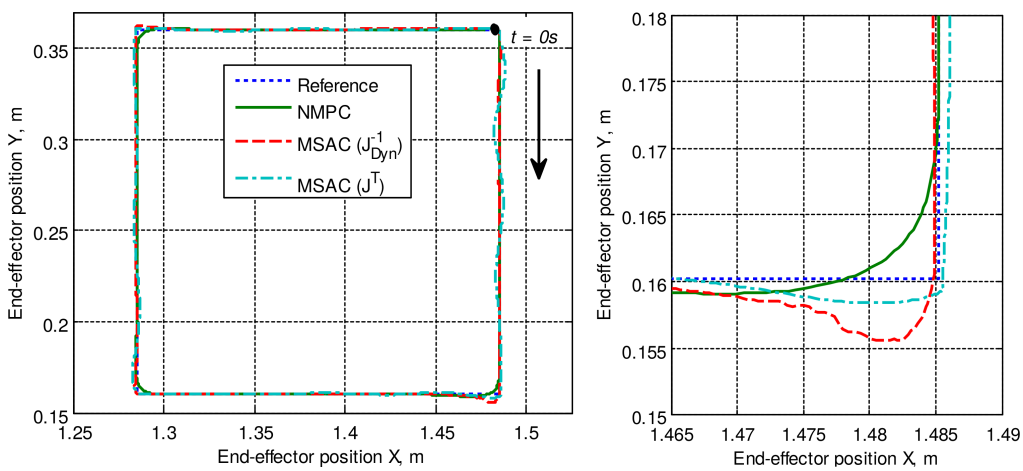

Figure 4: The end-effector position during the realization of the reference trajectory: the whole trajectory (left panel) and its first corner (right panel)

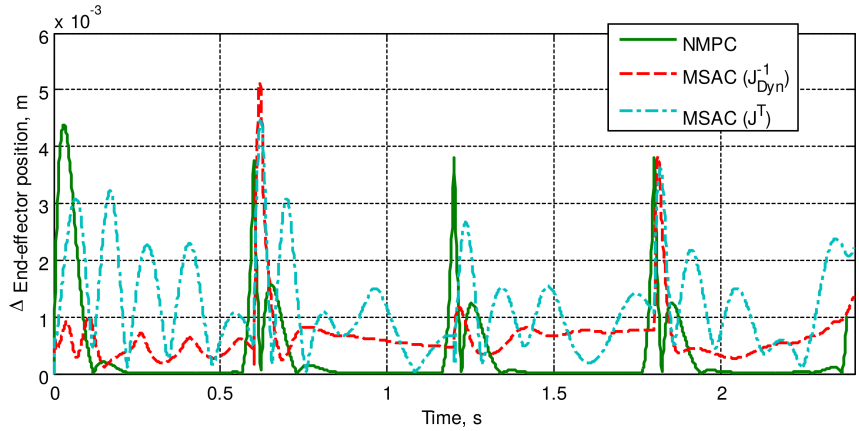

Figure 5: Difference between the reference end-effector trajectory and end-effector position obtained from the numerical simulations

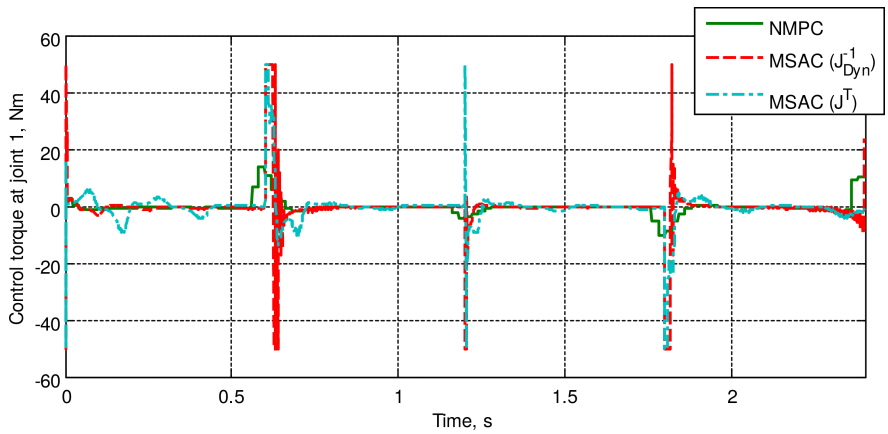

Figure 6: The control torque applied in the first joints of the manipulator during realization of the reference trajectory

The results of numerical simulations presented in this paper show that the proposed control system based on NMPC performs better than MSAC. In each variant the control system was able to ensure proper realization of the selected reference trajectory. In case of the predictive control the end-effector begins to change its direction of motion before reaching the corner of the reference trajectory. Due to this fact total error in the trajectory realization is smaller for NMPC. As expected, use of the inverse of the dynamic Jacobian in MSAC gives better results than the classical version of this method (with the transpose of the geometric Jacobian). In case of MSAC changes of the control torques applied in

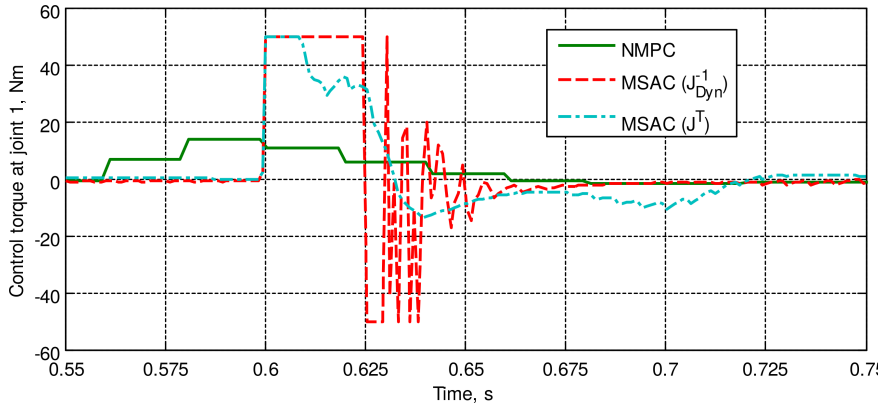

Figure 7: The control torque applied in the first joint of the manipulator during motion of end-effector at the first corner of the square

the manipulator joints during the motion of the end-effector through the corners of the reference trajectory are very rapid and maximal allowed values of these torques are reached (50 Nm). In case of NMPC changes of the control torques are gentle and maximal values are much lower. Unfortunately, computational cost of the predictive control is much higher than the computational cost of adaptive control (even for the case with the dynamic Jacobian). For NMPC computational cost depends on the selected length of prediction horizon. High computational cost of this method may be a serious problem for the application of this method in one of planned space missions, in which it is considered to use a 6 DoF manipulator.

5. Conclusions

In this paper we have presented a concept of the control system for a manipulator mounted on a satellite. This control system is composed of two modules: the trajectory planning module and the model predictive controller (responsible for ensuring precise realization of the planned trajectory despite disturbances and non-perfect knowledge of the mass and geometrical properties of the satellite-manipulator system). Numerical simulations were performed for the simplified planar case. These simulations showed that the results obtained with Non-linear Model Predictive Controller (NMPC) are better than the results obtained with the adaptive control. In the analyzed case the use of the predictive controller results in lower maximal values of the control torques applied in the manipulator joints. However, computational cost of the predictive control is higher than the computational cost of adaptive control.

References

[1] E.F. CAMACHO and C. BORDONS: Model predictive control. 2nd ed.. London, Springer, 2007.

[2] A. ELLERY, J. KREISEL and B. SOMMER: The case for robotic on-orbit servicing of spacecraft: spacecraft reliability is a myth. *Acta Astronaut.*, **63** (2008), 632–648.

[3] A. FLORES-ABAD, *et al*.: A review of space robotics technologies for on-orbit servicing. *Prog. Aerosp. Sci.*, **68** (2014), 1–26.

[4] W. LEY, K. WITTMANN and W. HALLMANN [Eds.]: Handbook of space technology. Singapore, Wiley, 2009.

[5] J. L. JUNKINS and H. SCHAUB: An Instantaneous Eigenstructure Quasivelocity Formulation for Nonlinear Multibody. *Dynamics. J. Astronaut. Sci.*, **45** (3) (1997), 279–295.

[6] E.G. KAIGOM, T.J. JUNG and J. ROSSMANN: Optimal Motion Planning of a Space Robot with Base Disturbance Minimization. In: 11th Symposium on Advanced Space Technologies in Robotics and Automation (ASTRA'2011). *Proceedings*. Noordwijk, The Netherlands, 2011.

[7] R. MCCOURT and C.W. DE SILVA: Autonomous robotic capture of a satellite using constrained predictive control. *IEEE/ASME Trans. Mechatronics*, **11** (6) (2006).

[8] M. ODA: Summary of NASDAs ETS-VII robot satellite mission. *J. Robot. Mechatron.*, **12** (4) (2000).

[9] T. RYBUS K. SEWERYN and J.Z. SĄSIADEK: Control system for free-floating space manipulator based on Nonlinear Model Predictive Control (NMPC). *J. Intell. Robot. Syst.*, **85**(3) (2017), 491–509

[10] T. RYBUS, K. SEWERYN and J.Z. SĄSIADEK: Nonlinear Model Predictive Control (NMPC) for free-floating space manipulator. In: *Aerospace Robotics III, GeoPlanet: Earth and Planetary Sciences*. Ed. J. Z. Sąsiadek, 2018, Springer (in press).

[11] T. RYBUS, K. SEWERYN and J.Z. SĄSIADEK: Układ sterowania manipulatorem satelitarnym wykorzystujący algorytm sterowania predykcyjnego. In: 14th National Conference on Robotics (14. Krajowa Konferencja Robotyki). *Proceedings.* Polanica Zdrój, Poland, 2016.

[12] T. RYBUS, K. SEWERYN and J.Z. SĄSIADEK: Trajectory optimization of space manipulator with non-zero angular momentum during orbital capture maneuver. In: AIAA Guidance, Navigation, and Control Conference. *Proceedings*. San Diego, USA, 2016.

[13] T. RYBUS, *et al*.: Numerical simulations and analytical analysis of the orbital capture maneouvre as a part of the manipulator-equipped servicing satellite design. In: 17th International Conference on Methods and Models in Automation and Control (MMAR2012). *Proceedings*. Międzyzdroje, Poland, 2012.

[14] K. SEWERYN and M. BANASZKIEWICZ: Optimization of the trajectory of a general free-flying manipulator during the rendezvous maneuver. In: AIAA Guidance, Navigation, and Control Conference and Exhibit. *Proceedings*. Honolulu, Hawaii, USA, 2008.

[15] S.V. SHAH, *et al*.: Energy optimum reactionless path planning for capture of tumbling orbiting objects using a dual-arm robot. In: 1st International and 16th National Conference on Machines and Mechanisms. *Proceedings*. IIT Roorkee, India, 2013.

[16] M. SHAN, J. GUO and E. GILL: Review and comparison of active space debris capturing and removal methods. *Prog. Aerosp. Sci.*, **80** (2016), 18–32.

[17] S. ULRICH and J. SASIADEK: Modified simple adaptive control for a two-link space robot. In: IEEE American Control Conference. *Proceedings*. Baltimore, Maryland, USA, 2010.

[18] D.M. WALTZ: On-orbit Servicing of Space Systems. Malabar, Kriger, 1993.